HORIZON 2020

HORIZON 2020 RESEARCH AND INNOVATION FRAMEWORK PROGRAMME OF THE EUROPEAN ATOMIC ENERGY COMMUNITY

Nuclear Fission and Radiation Protection 2018 (NFRP-2018-4)

Project acronym: **SANDA**

Project full title: **Solving Challenges in Nuclear Data for the Safety of European Nuclear facilities**

Grant Agreement no.: **H2020 Grant Agreement number: 847552**

Workpackages: ***WP1***

Identification N°: ***D1.3***

Type of document: ***deliverable***

Title of milestone: Report on the performances of new devices for precise study of fission products and their decay in view of measurements

Dissemination Level: ***PU***

Reference:

Status: ***Achieved***

Actual Delivery date: 31 March 2022

Comments:

	Name	Partner	Date	Signature
Prepared by:	D. Doré	3	03-30-2022	
WP leader:	M. Kerveno	5	03-30-2022	
IP Co-ordinator:	E. González	1	03-31-2022	Signed by E. Gonzalez at 31/03/2022 with certificate from AC Sector Público

SANDA WP1, Subtask 1.1.2.
Report for the Deliverable D.1.3

Introduction

The deliverable 1.3 is a report on the performances of new devices for precise study of fission products and their decay in view of measurements. Three sections composed the present document: 1- Improvements of the FALSTAFF spectrometer for the study of 235U fission fragment at NFS (SPIRAL2/GANIL, Caen), 2- New version of the BELEN detector for beta-delayed neutron spectra and probability (Pn) measurements, 3- New facility at CEA/LNE-LNBH for half-life measurements with 0.1% of uncertainty. References are listed at the end of each section.

1. Improvements of the FALSTAFF Spectrometer

The FALSTAFF spectrometer was developed to characterize fission fragments (FF) from neutron induced fission on actinides and determine the neutron multiplicity according to the mass of the fragments [1,2]. The final experimental setup will be composed of two arms (Fig. 1.1) but only one has been built and improved up to now (Fig. 1.2).

Method

The FF mass before neutron evaporation is obtained via the 2V (Double Velocity) method. It requires the measurement of both fragment velocities in coincidence. The velocity is determined with two time-of-flight (ToF) Secondary Electron Detectors (SeD). Each detector gives the arrival time and position of a particle on the detector. A SeD is made up of an emissive foil followed by an accelerating grid and a Multi-Wire Proportional Chamber (MWPC) detector. When a fragment crosses the emissive foil, electrons are produced, and thanks to an electric field, are accelerated and detected by MWPC detector. The requested time and position resolutions are 120 ps and 2 mm. The FF mass after neutron evaporation is obtained with the EV (Energy-Velocity) method. Then, in addition to the velocity information, the kinetic energy value of the fragment is required. An axial ionization chamber provides the residual energy. The expected resolution is ~1%.

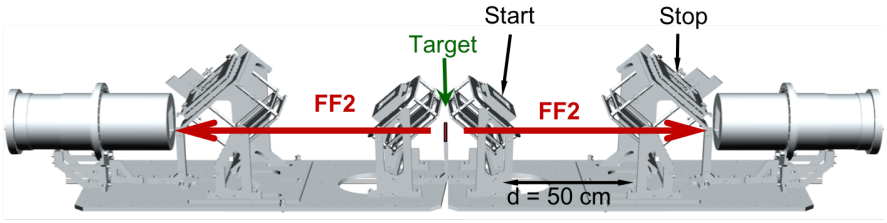

Fig. 1.1 Sketch of the two arms of the FALSTAFF spectrometer.

Tests and validation

The validation of the setup was expected in 2018 from an experiment performed at the Orphée reactor (Saclay) for the study of thermal neutron induced fission of ^{235}U. Unfortunately, the desired target has not been used due to administrative problem and the replacement target had a too small amount of ^{235}U. In addition, the intensity of the neutron beam was much smaller than expected. Nevertheless, some problems with one of the TOF detectors were identified.
In 2019 the detector was replaced. Results obtained with a ^{252}Cf source were satisfactory and allowed us to submit a proposal for the study of fast neutron induced fission of ^{235}U to the GANIL/NFS PAC. The proposal was accepted in September 2019 and preliminary results of this experiment will be presented in the report associated to the deliverable 2.13 and the milestone 2.3.

Since the beginning of the SANDA contract and particularly in 2021, many improvements have been brought to the setup.

- Another new TOF detector, identical to the previous one, was installed. They are larger than the ones used before 2019 and have a more uniform efficiency.

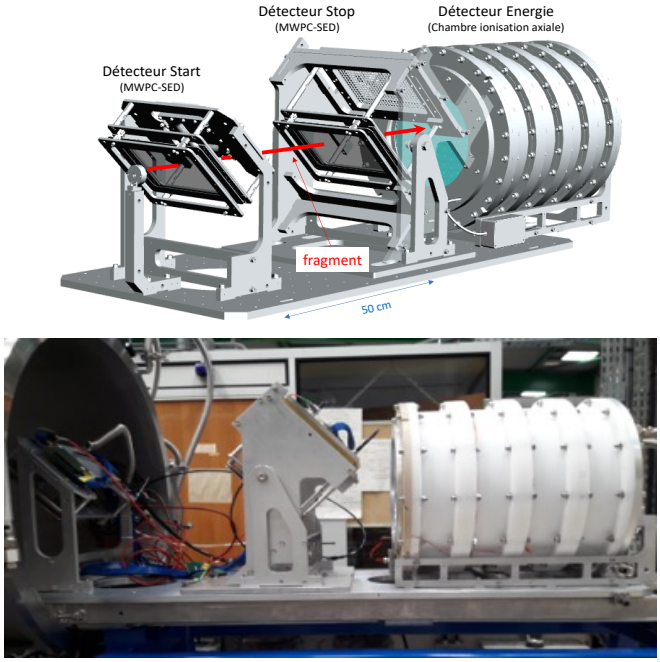

Fig. 1.2 Diagram and picture of the first arm of FALSTAFF (2018 version).

- The Frisch grid of the axial ionization chamber was replaced in order to increase the efficiency. Instead of a plane of wires, a mesh made of bronze wires of 80 mm diameter spaced by 0.93 mm was used.

- Pre-amplifier signals of the anode and grid of the ionization chamber have been changed.

- The DAQ system was upgraded. A new card (BEAST) which distributes the timestamp to the VME system and the GET system was tested and is now routinely used. Thanks to this new system, the energy-time subsystem (VME) and the position subsystem (GET) are perfectly synchronized.

- A new ^{252}Cf source was bought, reducing the time needed for the tests.

- Results of an experiment performed at Lohengrin (ILL reactor, Grenoble) concerning the energy loss of fragments in mylar foils [3] have been included in simulations and experimental data analysis codes. Note, that fragment energy measured in the axial chamber has to be corrected to take into account the chamber window and the emissive foil of the stop detector in order to have the velocity and the energy at the same point.

Many tests have been performed in 2021 after these modifications. Some preliminary results are shown in Fig. 1.3 and Fig. 1.4. Experimental results (in blue) are compared to simulations (in red). Simulations have been performed in the GEANT4 framework using the fission observables from the FIFRELIN [4] code as input. The agreement between simulations and data is rather good (Fig. 1.3). The fragment mass distribution after evaporation (right panel of Fig. 1.4) has the expected trend. The valley is more pronounced than in the distributions obtained with original detectors [5]. However, there is mass shift

probably due to a small velocity shift or a problem with the energy calibration. These aspects will be further investigated soon. The spectrometer was moved from Saclay to GANIL mid-September 2021.

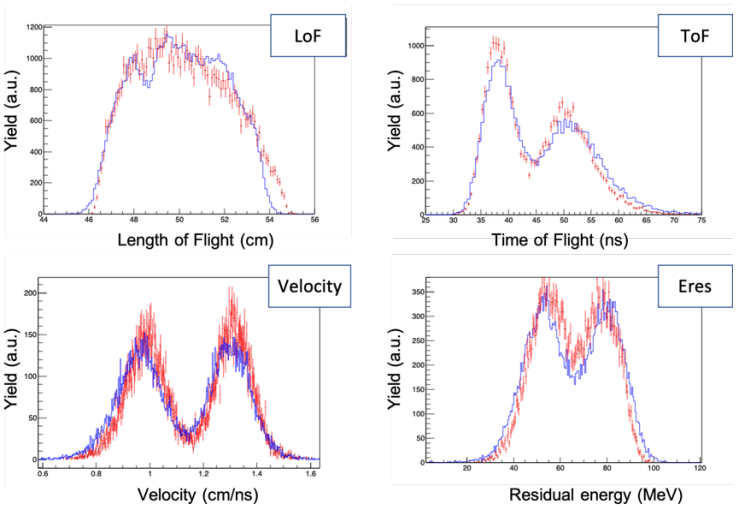

Fig. 1.3 Comparisons between experimental (blue curves) and simulations (red curves) for the Length-of-Flight, Time-of-Flight, velocity and residual energy distributions.

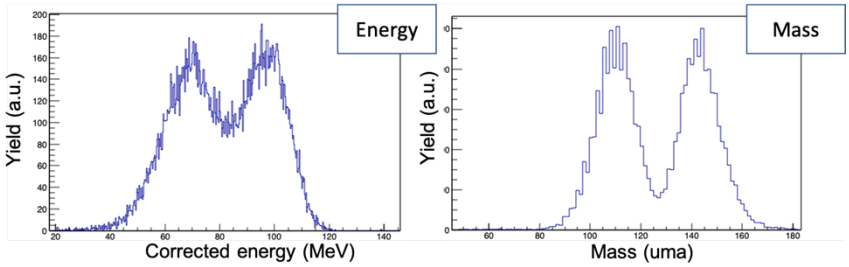

Fig. 1.4 Reconstructed corrected energy and fragment mass distributions.

Beginning 2022, FALSTAFF was put close to the VAMOS spectrometer [6] to perform an experiment in March 2022 (out of the SANDA project) in order to evaluate its the ability to determine the charge of fragments. One of the fragments of the ^{238}U beam on carbon target reaction at 5.8 MeV/u will be fully identified in VAMOS. The partner fragment will be slowed down to reach the fragment velocity in direct kinematics and will be detected in FALSTAFF. A scheme of the setup is presented in Fig 1.5. Results will allow to train a neural network in order to be able to identify fragment nuclear charge in future experiments.

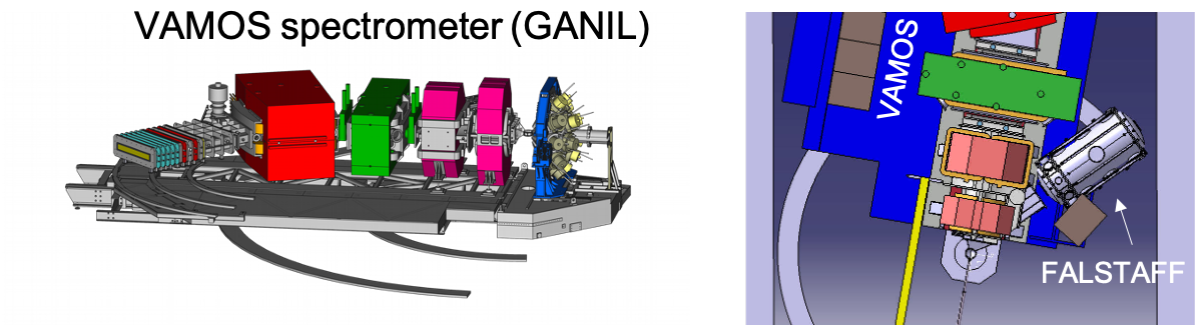

Fig. 1.5 VAMOS and VAMOS + FALSTAFF schemes.

Conclusions

Many improvements have been brought to the FALSTAFF setup. Results show a rather good agreement with simulations. Thanks to the experiment combining FALSTAFF and VAMOS, the nuclear charge identification in FALSTAFF can be foreseen. Then, the first arm of FALSTAFF is ready for the experiment at NFS planned for November 2022. This experiment will provide fission fragment distributions over a large range of incident neutron energy.

References

[1] D. Doré et al., NuclearDataSheets 119, 346 (2014).

[2] Q. Deshayes et al., EPJ Web of Conferences 239, 0512 (2020).

[3] T. Materna et al., NIMB 505 (2021) 1-16.

[4] O. Litaize et al., Eur. Phys. J. A, vol 51, no177, 991-4 (2015).

[5] D. Doré et al., EPJ Web of Conf., 211, 01002 (2019).

[6] D. Ramos et al., Phys. Rev. C 97, 054612 (2018).

2. New version of the BELEN detector for beta-delayed neutron spectra and probability (Pn) measurements

BELEN (BEta-deLayEd Neutron detector) is a detector-design aiming at measuring beta-delayed neutrons emission probabilities of nuclides of interest in nuclear technology and nuclear physics. In a very simplistic way, it consists in a set of rings made of thermal neutron detectors (He-3) embedded in a High-Density Polyethylene (moderator) matrix. So far, the BELEN concept has been used in several experimental campaigns at GSI, JYFL, and RIKEN, making use of a digital electronic trigger-less data acquisition system (Gasific).

All BELEN versions used so far have been designed and constructed with two main design criteria, namely a) attain the largest neutron detection efficiency compatible with, b) a flat energy-response in a predefine range of neutron energies. Therefore, each BELEN detector, has been acting as a neutron-counter with a flat response to a given neutron energy range. In the framework of this project, new design criteria have been introduced, so that the detector have spectrometric capabilities.

Neutron spectrometry

A wide-spread technique for neutron energy measurement is the so called “Bonner spheres spectrometer”. It consists in a set of polyethylene spheres of different diameters with a thermal neutron detector in their center. Due to the different moderator depths, each sphere is sensitive to a different neutron energy range. In order to have a good energy resolution, sets of 5-14 spheres of different diameter are usually used to determine the energy spectrum of neutron fields up to a few hundreds of MeV. As a first approximation, each ring of BELEN [1-2] can be considered as equivalent to a Bonner sphere. Therefore, one would expect to extract some spectrometric information from BELEN.

BELEN versions

BELEN has already been used at JYFL, GSI and RIKEN. The settings of every single version have been made to meet the particular specifications of each facility and experiment. This just-in-time approach is followed to optimize the performance of the detector being used. The number of tubes, the number and location of the groups of counters (usually in the form of rings), the type of tubes in each group, and the spacing among tubes and groups, has been designed by Monte Carlo simulations in order to achieve the best compromise between high efficiency and flat response for the neutron’s energy range of each measurement.

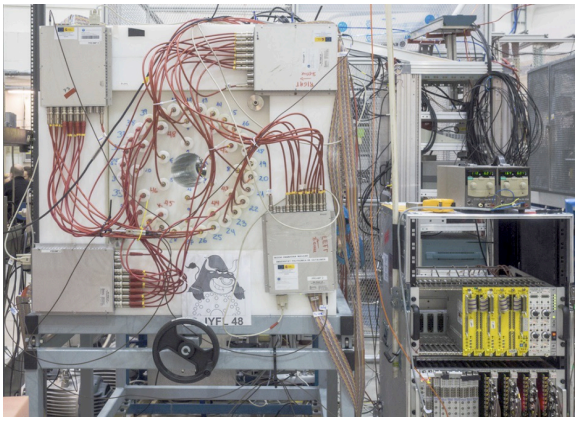

Fig. 2.1 BELEN-48 used at JYFL in Nov 2014.

The first two BELEN versions were made of 20 counters (BELEN-20), distributed in two rings, and were used in two experiments at JYFL in 2009 and 2010. The next design, BELEN-30, was employed at GSI in 2011. It was composed by 30 counters (3 rings). Two BELEN-48 versions (3 rings, different central hole

each), similar to the design for FAIR [1] as part of the NUSTAR [2]-DESPEC [3] setup, were used at JYFL in 2014 (see Fig. 2.1). BELEN-48 [3] is the accepted version for Nustar-DESPEC at FAIR.The last BELEN version is part of a larger delayed neutron detector (140 He-3 tubes distributed in 7 groups), known as BRIKEN [4-5] (BELEN for RIKEN). It has been used in a long experimental campaign at RIKEN.

In terms of spectrometric capabilities, BELEN-20, BELEN-30 and BELEN-48 are expected to have no, or very poor, energy responses. They are made of only two or three rings, making them equivalent to a set of 2 or 3 Bonners spheres, which is not enough to obtain energy spectra. Therefore, only BRIKEN could provide neutron energy information.

BRIKEN neutron-energy capabilities

BRIKEN is being used in a long-lasting (2016-2021) experimental campaign at RIKEN. It is made of 140 He-3 detectors embedded in polyethylene using a seven "pseudo-ring" geometry (see Fig. 2.2).

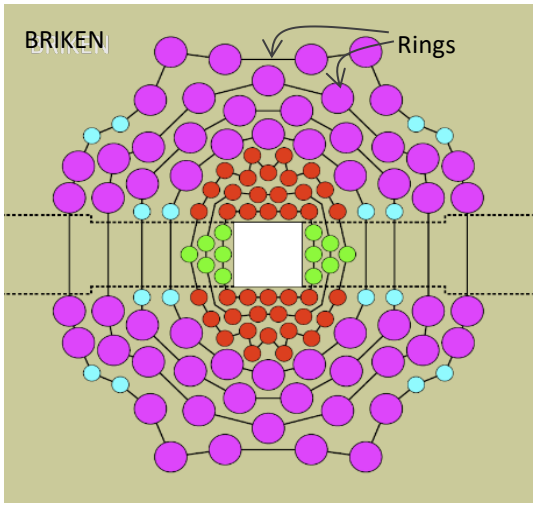

Fig. 2.2 BRIKEN detector geometry.

Several radionuclides, and a neutron source, were used for testing, experimentally, the neutron energy sensitivity per ring. These nuclides were selected due to the differences in their neutron energy spectrum (see Table 2.1).

Table 2.1 BRIKEN. Magnitudes of neutron spectra for selected nuclides.

Nuclide	$Q_{\beta 1}$, MeV	Mean Energy, MeV
Ge-85	4.66	0.69
Cu-77	5.61	0.79
Cu-78	6.22	0.80
Ga-83	8.09	1.01
Cf-252	-	2.13

Each ring shows a different response to the neutron spectrum's mean and end-point (~$Q_{\beta 1}$) energies (see Fig. 2.3). Rings are ordered using its radius, ring number 1 is the one located closest to the center of the detector). One can conclude that, even though BRIKEN has not been designed with spectrometric response in mind, it shows sensitivity to neutron energy spectra.

Basic design criteria of a spectrometric BELEN

In order to design a new version of BELEN with spectrometric response, a basic criterium was imposed: attain a mean neutron detection efficiency of at least 50% for energies up to 5 MeV using the minimum

number He-3 tubes. Since the energy spectrum of the neutrons will be measured, the “flat energy-response in a predefine range of neutron energies” criterium could be relaxed.

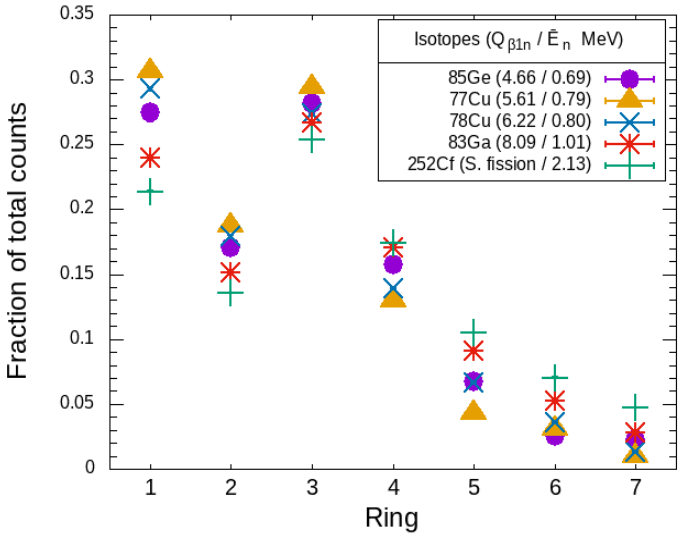

Fig. 2.3 BRIKEN energy sensitivity per ring for selected radionuclides.

Based on our experience in beta-delayed neutron detectors design, construction and exploitation, we have decided to work with He-3 tubes of 60 cm length, 2.54 cm diameter and a pressure of 8 atm. These tubes have a good intrinsic detection efficiency for thermal neutrons, and a good separation between “noise” signals (micro-discharges, gammas, …) and neutron signals. On top of that, those are the most common tubes in our current stock. Additionally, the high-density polyethylene (HDPE, 0.95 gr/cm^3) matrix was set to have a cross-section of 90x90 cm^2 with a central hole of a radius of 4.5 cm. The polyethylene block dimensions are a good compromise between detector weight and neutron-background rejection. The overall dimensions are compatible with the expected space available in the future DESPEC hall at FAIR.

Procedure to design a spectrometric BELEN

Starting with 48 He-3 tubes, an iterative process of distributing the tubes in four or more rings was carried out. For every configuration the energy response and mean neutron detection efficiency was computed by Montecarlo simulations using ParticleCounter [6] an application based on GEANT4 (version 10.01.03) including neutron HP data and thermal scattering data libraries [7-10]. If the overall efficiency was below the 50% limit, or the energy response was poor, a new set of tubes was added.

With a set of 62 tubes distributed in 6 rings, BELEN-62, (See Fig. 2.4 and Table 2.2), a good compromise of energy response (Fig. 2.5) and total efficiency (Fig. 2.6) is reached. Neutron detection efficiency is in average 51% for neutron energies up to 5 MeV, and presents a rather flat behavior up to 2.5 MeV. Even though the “flat energy response” criterium was not imposed, the resulting flatness is comparable to that of BELEN-48.

In order to further improve the energy response, an extra ring would be needed. But, adding an extra ring, will require more than 20 extra He-3 tubes. Therefore, we consider 62 as the number of tubes to reach a good balance among performance and cost.

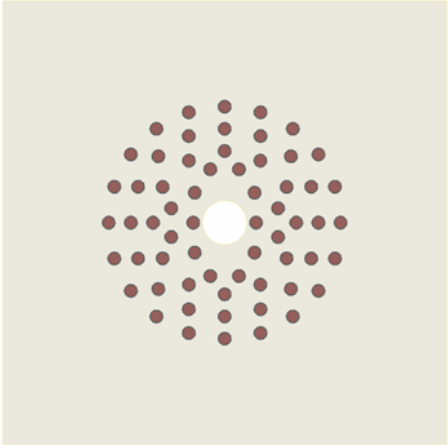

Fig. 2.4 BELEN-62 detector geometry.

Table 2.2. BELEN-62 rings properties.

Ring	Tubes	R, cm
1	2	6.38
2	4	8.58
3	8	11.20
4	12	14.50
5	16	19.00
6	20	23.50

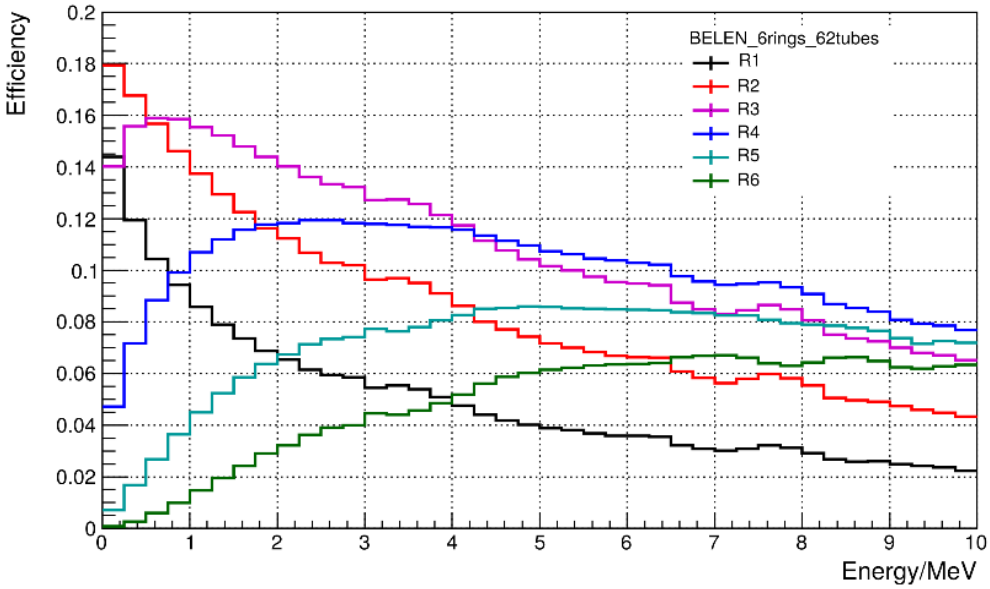

Fig. 2.5 BELEN-62 energy response.

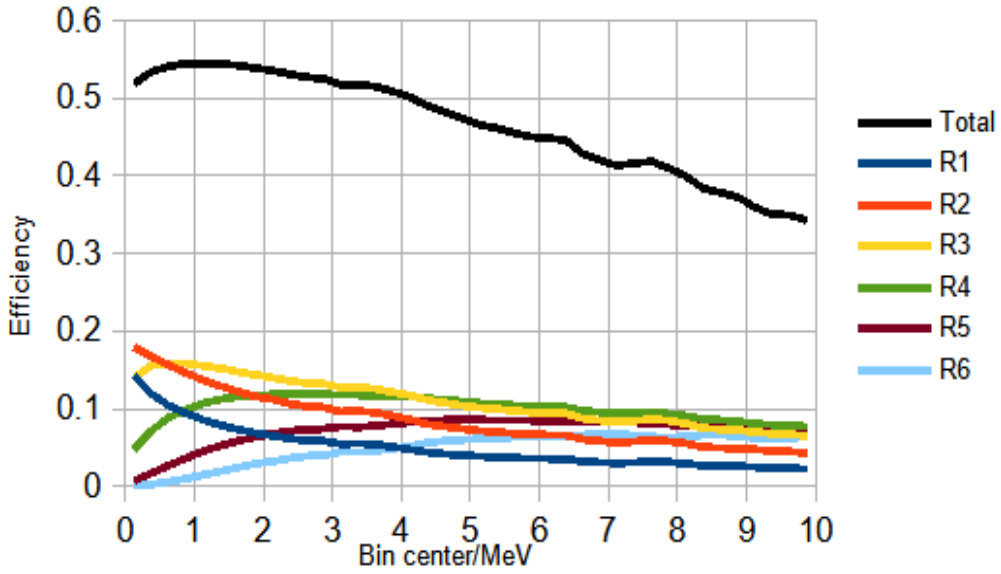

Fig. 2.6 BELEN-62 neutron detection efficiency.

Spectrometric performance of BELEN-62

A set of radionuclides, selected among the standards recommended in literature [11], and a neutron source (see Table 2.3) were used to test energy response of the new design. The energy spectra of each radionuclide were taken from ENDF/B-VIII.0 [12]. For each radionuclide, the counts on each He-3 tube were obtained using Geant4.

Table 2.3 BELEN-62. Neutron spectrum magnitudes of selected nuclides.

Nuclide	$Q_{\beta n}$, MeV	<E>, MeV
Cf-252	---	2.13
Br-88	1.922	0.2515
Rb-94	3.452	0.4424
Rb-95	4.883	0.5295
I-137	2.001	0.6298

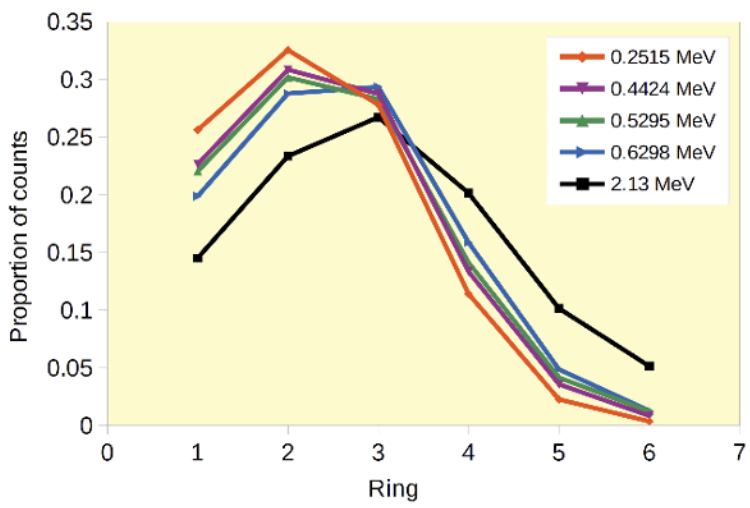

Fig. 2.7 BELEN-62 energy sensitivity per ring for selected radionuclides.

As when analyzing BRIKEN, the counts-per-ring were used as a first indicator of the spectrometric capabilities of the detector. The new design presents a good energy sensitivity per ring (see Fig. 2.5). In order to analyze the spectral sensitivity of the new design, energy spectra were obtained unfolding the detector's counts. A Bayesian unfolding method [13] was used to reconstruct the "measured" spectra. The algorithm is iterative and requires an a-priori information (initial spectrum guess). As initial educated guesses, a Maxwellian spectrum (T=2 MeV) was used for Cf-252, while a simple constant beta-strength spectrum was used for the beta-delayed neutron emitters. A good agreement is found between the unfolded spectra and the expected ones (see Fig. 2.8 to Fig. 2.12 and Table 2.4).

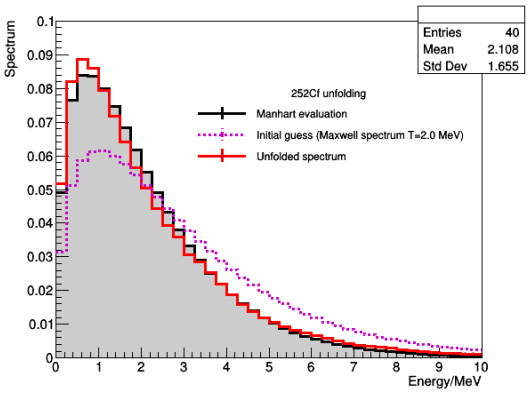

Fig. 2.8 BELEN-62. Cf-252 spectrum.

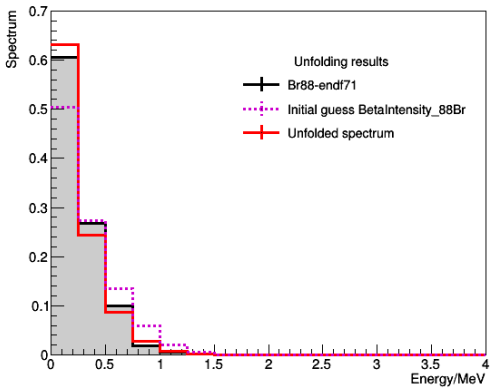

Fig. 2.9 BELEN-62. Br-88 unfolded spectrum.

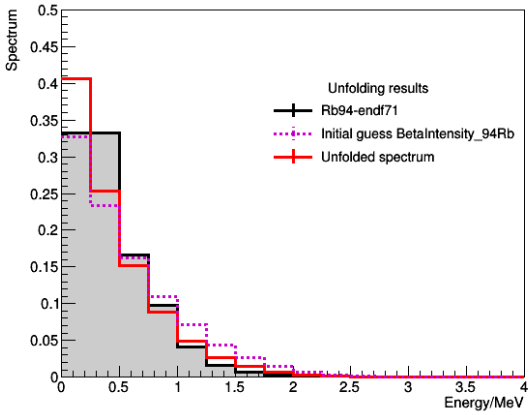

Fig. 2.10 BELEN-62. Rb-94 unfolded spectrum.

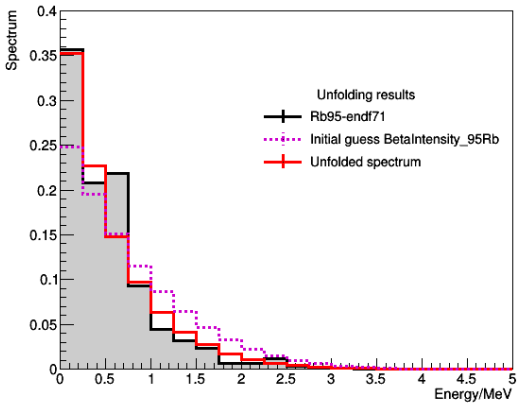

Fig. 2.11 BELEN-62. Rb-95 unfolded spectrum.

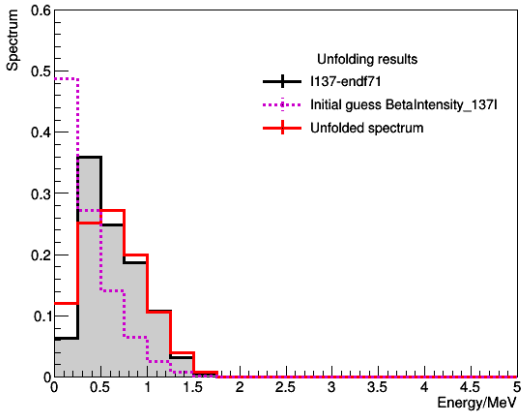

Fig. 2.12 BELEN-62. I-137 unfolded spectrum.

Table 2.4 Ratio of expected to unfolded mean energies.

Nuclide	Ratio <E>
Cf-252	1.019
Br-88	1.033
Rb-94	1.032
Rb-95	1.091
I-137	1.023

Concluding remarks

A new device, BELEN-62, for precise study of fission products and their decay for future measurements has been designed. BELEN-62 has a mean neutron detection efficiency larger than 50% for neutron energies up to 5 MeV. For neutron energies up to 2.5 MeV, the efficiency has a flatter behavior than BELEN-48.

BELEN-62 has good spectrometric capabilities. The mean energies are well reproduced. The unfolded spectra are a good smoothed representation of the expected ones. This makes BELEN-62 a unique device to measure simultaneously probabilities of multi-neutron emissions, and spectral information.

Acronyms

GSI: GSI Helmholtzzentrum für Schwerionenforschung, Darmstadt, Germany
JYFL: Accelerator Laboratory, University of Jyväskylä, Finland
RIKEN: Radioactive Isotope Beam Factory (RIBF), Nishina Center for Accelerator-Based Science, Wako, Japan

References

[1] A. Riego. "Design of the BELEN detector for wide energy range with flat and high detection efficiency", PhD Thesis report, 2016, http://hdl.handle.net/2117/96361

[2] J.Agramunt, J.L.Tain, M.B.Gómez-Hornillos, A.R.Garcia, F.Albiol, A.Algora, R.Caballero-Folch, F.Calviño, D.Cano-Ott, G.Cortés, C.Domingo-Pardo, T.Eronen, W.Gelletly, D.Gorelov, V.Gorlychev, H.Hakala, A.Jokinen, M.D.Jordan…E.Valencia . "Characterization of a neutron–beta counting system with beta-delayed neutron emitters", NIM A 807 pag. 69-78, 2016, https://doi.org/10.1016/j.nima.2015.10.082

[3] F. Calviño, G. Cortes et al. "TDR BEta-deLayEd Neutron detector", 2014, https://fair-center.eu/user/experiments/nustar/documents/technical-design-reports last access 2022/02/28

[4] A. Tarifeño-Saldivia et al. "Conceptual design of a hybrid neutron-gamma detector for study of beta-delayed neutrons at the RIB facility of RIKEN", JINST 12 P04006, 2017, https://doi.org/10.1088/1748-0221/12/04/P04006

[5] A.Tolosa-Delgado, J.Agramunt, J.L.Tain, A.Algora, C.Domingo-Pardo, A.I.Morales, B.Rubio, A.Tarifeño-Saldivia, F.Calviño, G.Cortes, N.T.Brewer, B.C.Rasco, K.P.Rykaczewski, D.W.Stracener, J.M.Allmond, R.Grzywacz, R.Yokoyama, M.Singhd…B.Moonw. "Commissioning of the BRIKEN detector for the measurement of very exotic beta-delayed neutron emitters", NIM A 925 pag. 133-147, 2019, https://doi.org/10.1016/j.nima.2019.02.004

[6] https://www.particlecounter.net/ last access 2022/02/28

[7] S.Agostinelli et al. "Geant4—a simulation toolkit", NIM A 506 pag. 250-303, 2003, https://doi.org/10.1016/S0168-9002(03)01368-8

[8] J. Allison et al. "Geant4 developments and applications", IEEE Transactions on Nuclear Science 53-1 pag. 270 – 278, 2006, https://doi.org/10.1109/TNS.2006.869826

[9] J.Allison et al. "Recent developments in Geant4", NIM A 835 pag. 186-225, 2016, https://doi.org/10.1016/j.nima.2016.06.125

[10] https://geant4.web.cern.ch/ last access 2022/02/28

[11] J. Liang et al. "Compilation and Evaluation of Beta-Delayed Neutron Emission Probabilities and Half-Lives for Z > 28 Precursors", Nuclear Data Sheets 168 pag. 1-116, 2020, https://doi.org/10.1016/j.nds.2020.09.001

[12] D.A.Brown et al. "ENDF/B-VIII.0: The 8th Major Release of the Nuclear Reaction Data Library with CIELO-project Cross Sections, New Standards and Thermal Scattering Data", Nuclear Data Sheets 148 pag. 1-142, 2018, https://doi.org/10.1016/j.nds.2018.02.001

[13] J.L. Tain, D. Cano-Ott. "Algorithms for the analysis of beta-decay total absorption spectra", NIM A 571 pag. 728-738, 2007, https://doi.org/10.1016/j.nima.2006.10.098

3. 3- New facility at CEA/LNE-LNBH for half-life measurements with 0.1% of uncertainty.

The Radioactivity Metrology Laboratory, Laboratoire National Henri Becquerel, is in the course of implementing a new measurement facility composed of a dedicated ionisation chamber and an automated sample changer in order to perform half-life measurements for a number of radionuclides important to the nuclear medicine community, as well as the nuclear industry, with uncertainties of 0.1%.

Initial testing, installation and operating conditions

Following an extensive study of available ionisation chamber suppliers, and feedback on the specific type of devices used in other metrology laboratories worldwide, a new IG11 ionisation chamber was ordered in late 2019 from Centronics, UK, which was delivered in June 2020, following the first lockdown period in France. Activities related to this task were able to start again only in September 2020, which included the necessary connections to the Keithley electrometer, purchased specifically for this chamber. In parallel, a design for a source holder consistent with the new chamber was completed during late 2020, and three copies were delivered in February 2021 (see Fig. 3.1).
Ambient background measurements, i.e. without a radioactive source in the chamber, were used to establish the working voltage. The high voltage was adjusted across the range from 0 V to -1000 V (see Fig. 3.2) and a working voltage of -650 V was established based on the visible plateau. A number of background measurements performed at this chosen voltage showed that the chamber response was as expected, with a background current of ~ 5×10^{-14} A.

Measurement repeatability and reproducibility

As the aim of this work is to have an automated measurement system, it is necessary to ensure the repeatability and reproducibility between measurements.

a) Measurement repeatability – no operator intervention

In order to test the repeatability of the ionisation chamber current measurements with the different sample holders, a series of 50 individual measurements of approximately 40 s, were automatically recorded, with a 5 mL ampoule of ^{137}Cs placed in a given source holder. Once placed in the chamber, the holder remains in place for the duration of the 50 measurements.

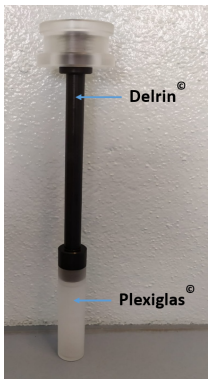

Fig. 3.1 The source holder for the Centronics IG11 ionisation chamber.

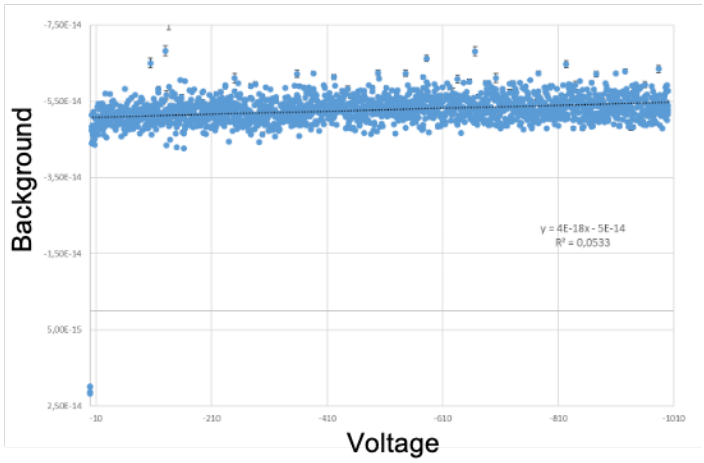

Fig. 3.2 Background measurement as the high voltage is varied.

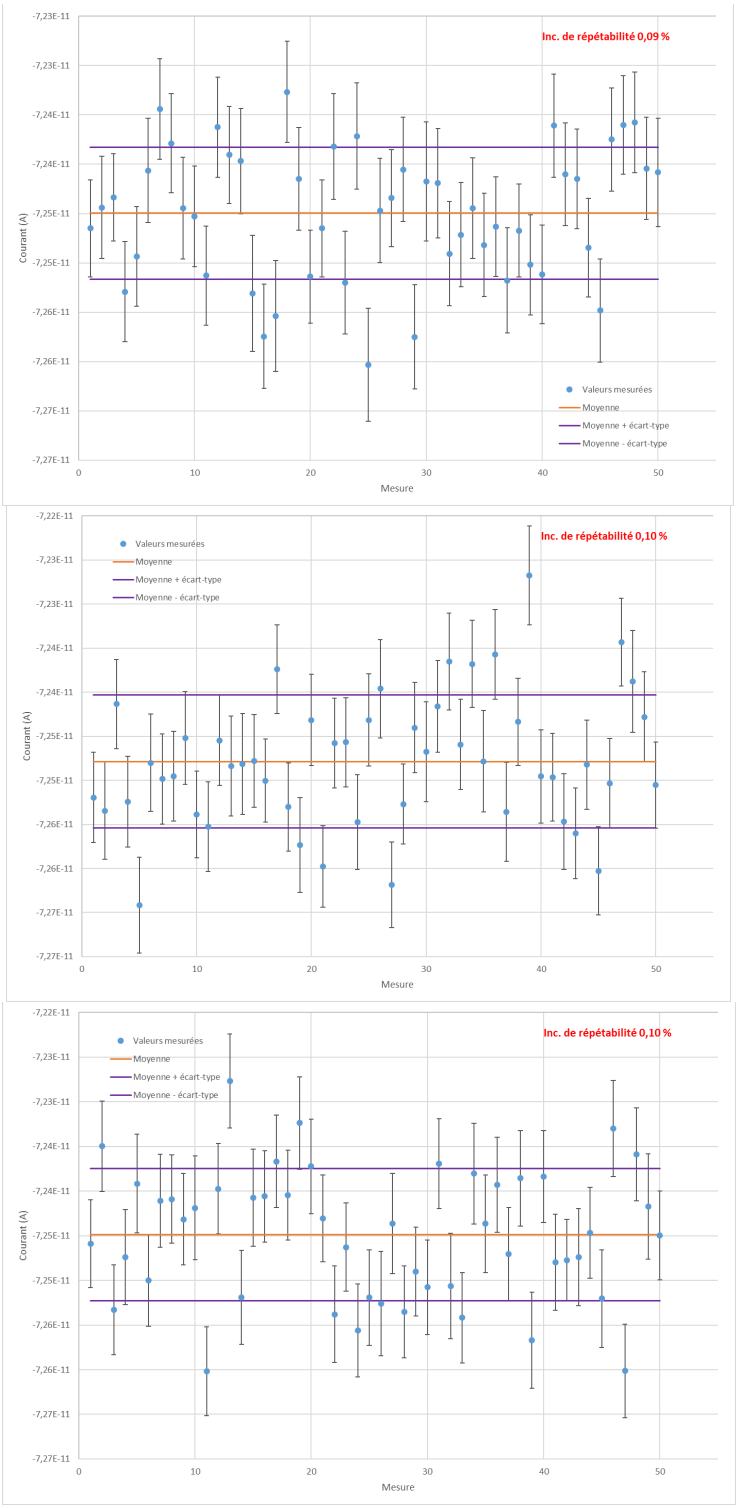

Fig. 3.3 Repeatability test with a 5 mL ^{137}Cs source solution and three different source holders (top, middle and bottom).

Three equivalent source holders were tested, with the same ^{137}Cs ampoule placed consecutively into each holder, prior to the series of 50 measurements being launched. The results for the three holders are shown in Fig. 3.3. An uncertainty of approximately 0.10% is observed in the variation across the ionisation chamber current measurements.

b) Measurement reproducibility –operator intervention

In order to test the reproducibility of the ionisation chamber current measurements with operator intervention, a series of 50 individual measurements of approximately 40 s were performed, with the three different sample holders and the same 5 mL ampoule of ^{137}Cs. Each holder was tested in turn, through a series of 50 measurements, with the systematic removal of the holder between each measurement. The results for the three holders are shown in Fig. 3.4. An uncertainty of no more than 0.12% is observed in the reproducibility across the ionisation chamber current measurements.

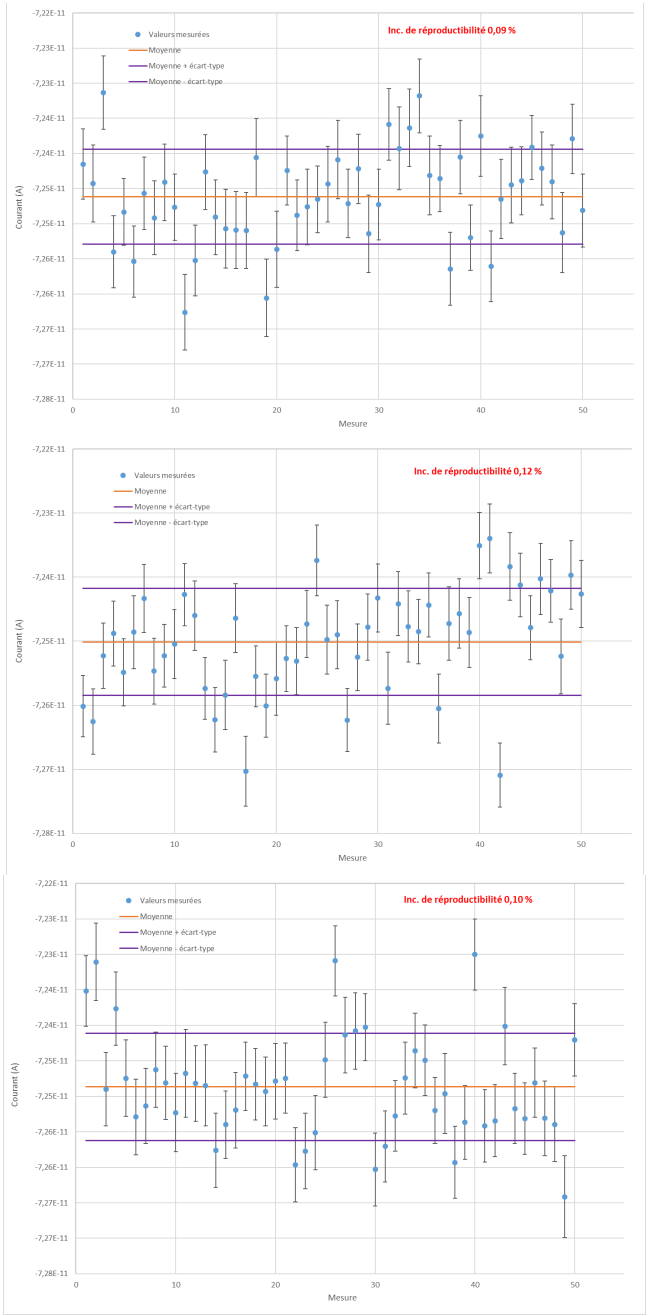

Fig. 3.4 Reproducibility test with a 5 mL ^{137}Cs source solution, three different source holders (top, middle and bottom), and systematic removal between measurements.

c) Measurement repeatability – different radioactive solutions and source holders

In order to ensure the equivalence between the three sample holders, a series of 40 s current measurements with six different test source solutions (^{125}I, ^{85}Sr, ^{57}Co, ^{152}Eu, ^{65}Zn and ^{137}Cs) were undertaken. Fig. 3.5 shows the results of these repeatability tests for the three source holders and the six source solutions. Variations from 0.1% to 1% were observed, with the highest variation of ~1% seen in the case of the ^{125}I solution. Due to the particularly low energy of the X- and γ-ray emissions associated to the electron capture decay of this radionuclide (from 4 keV to 35.5 keV), it is expected that this reproducibility test would be particularly sensitive for this radionuclide. Only minor variations in the sample holder construction will have a significant effect on the ionisation chamber response at such low emission energies.

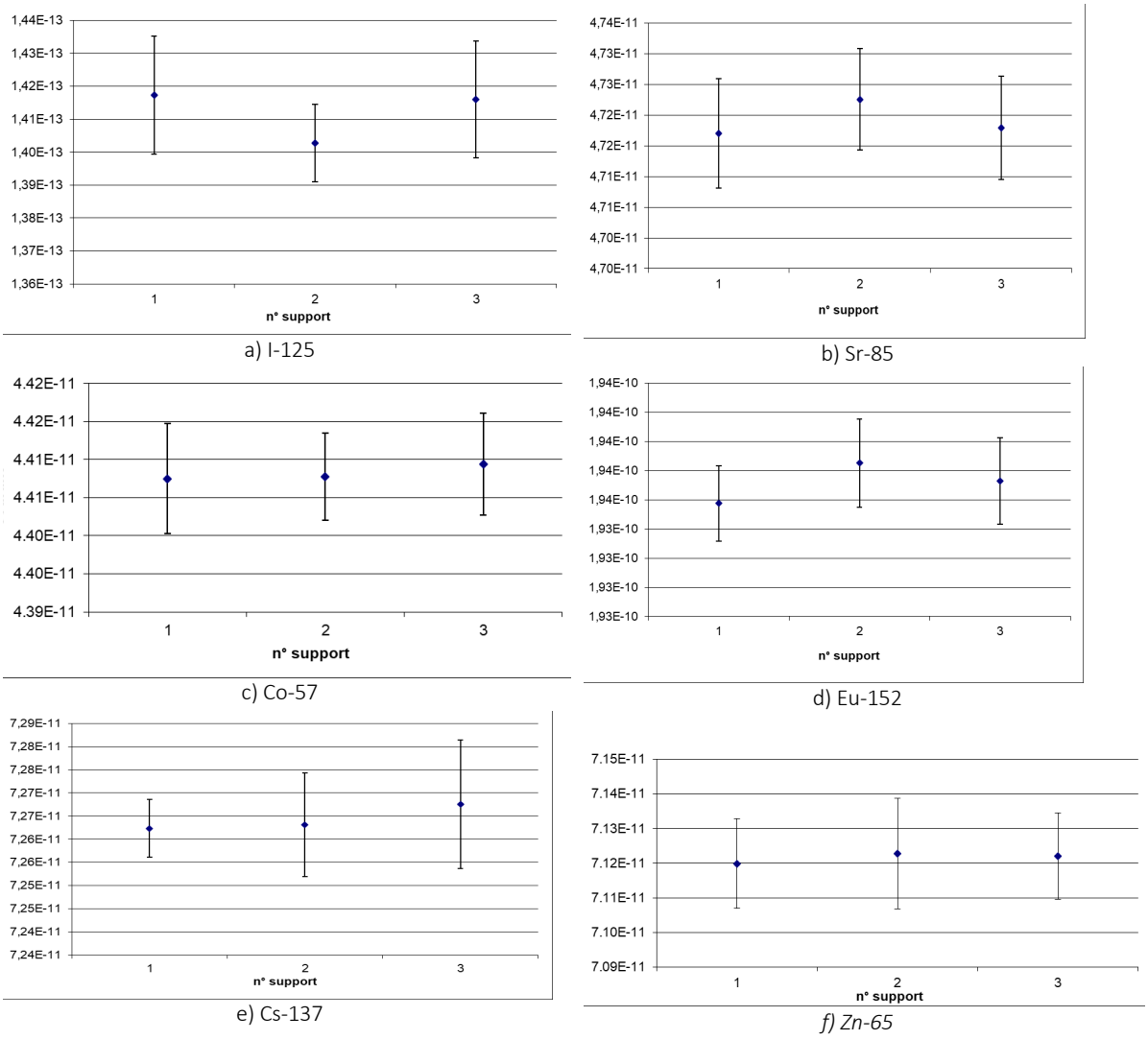

Fig. 3.5 Reproducibility tests for six sources and three sample holders.

Preliminary half-life measurement – ^{99m}Tc

Once the basic functionality of the ionisation chamber was established, the first measurement of a half-life was performed in late 2021. In order to test the robustness of the measurement chain and the analysis procedure, a measurement was performed which involved following the decay of the relatively short-lived radiopharmaceutical ^{99m}Tc. Given a half-life of approximately 6 h, the decay of the sample was followed for more than 100 h, i.e. almost 20 half-lives. Fig. 3.6 shows the decay of the measured ionisation chamber current with time and the associated fit to the experimental data. A Python code has been written to analyse the measured data, which yields a measured half-life value of 6.0068 h. The full uncertainty budget is still under evaluation, but an uncertainty of 0.0002 h has been calculated purely from the fitting procedure and the statistical uncertainty on the number of counts, i.e. 0.0033%. The final uncertainty will certainly be larger than this value.
As a comparison, two evaluated values for the half-life are available from the Decay Data Evaluation Project (DDEP) [1] which gives 6.0067 (10) h and the Evaluated Nuclear Structure Data File (ENSDF) [2] which gives 6.0072 (9) h. The ENSDF recommended value has been directly adopted from the measured value from the Physical Measurements Laboratory of the National Institute of Standards and Technology (NIST) [3].

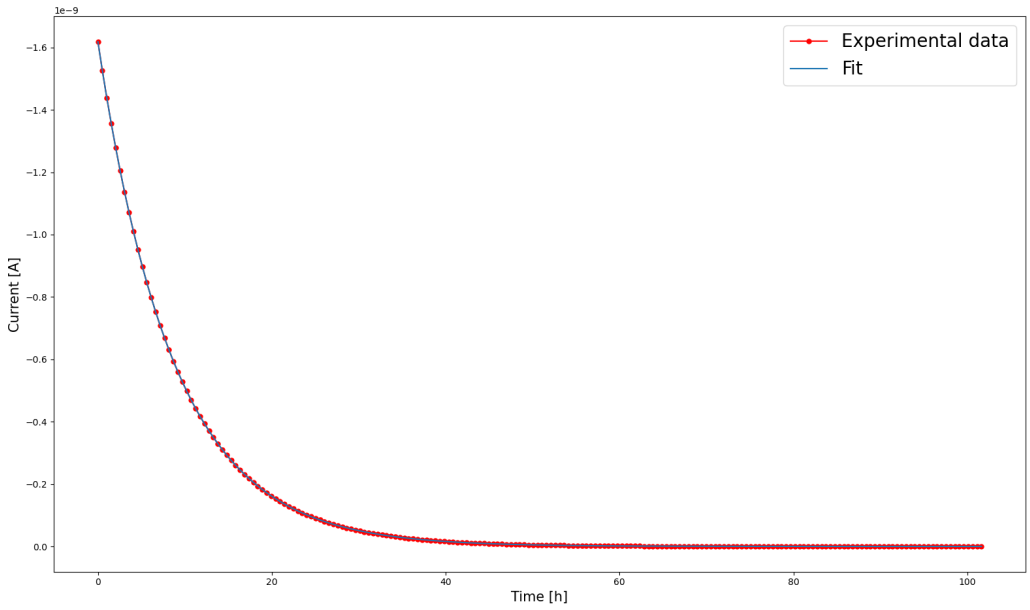

Fig. 3.6 Preliminary half-life measurement of ^{99m}Tc.

Preparatory simulations in order to allow automatic half-life measurements

In preparation for an automated measurement system, it is necessary to ensure that stored radioactive solutions close to the ionisation chamber will not interfere with the measurements and shielding requirements for the radioprotection of laboratory staff. Monte Carlo simulations with the PENELOPE-2018 code [4] were performed during summer 2021 in order to determine the thickness of the lead shielding that would be required in order to comply with our radioprotection regulations. Two views of the simulated geometry are shown in Fig. 3.7 where a carousel capable of storing 16 sources is clearly visible. A single source term for this carousel was then used to calculate the dose equivalent, *H*10 (µSv/h)*, at six different points in the laboratory, as shown in Fig. 3.8 and detailed in Table 3.1.

Table 3.1 Dose calculation points (as shown in Fig).

Position #	Description
1	Contact dose in the direction of the door
2	Dose at 50cm in the direction of the door
3	Dose at 100cm in the direction of the door
4	Contact dose perpendicular to the door
5	Dose at 50cm perpendicular to the door
6	Dose at 100cm perpendicular to the door

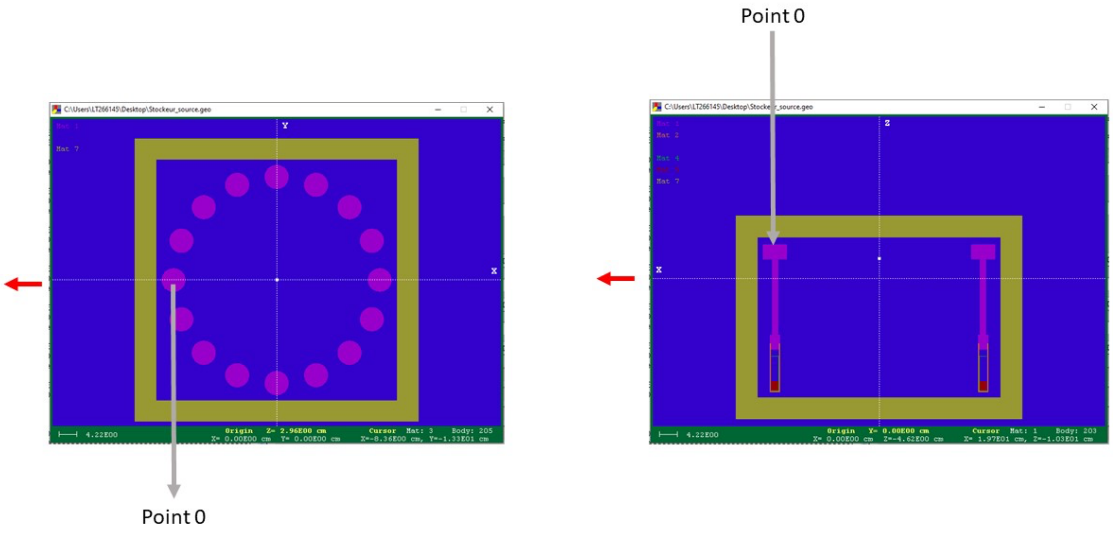

a) View from above *b) View from the side*

Fig. 3.7 Source stocker as simulated (the red arrow indicates the position of the ionisation chamber).

Two different values for the source term were studied, firstly assuming a 1 GBq ^{133}Ba equivalent source and the second with a 1 GBq ^{60}Co equivalent source. The results of the calculations are given in Table 3.2. The effect of the relatively low energy γ-rays from the ^{133}Ba decay (main γ-rays having energies between 53 keV and 384 keV) and the significantly higher energy γ-rays from the ^{60}Co decay (two main γ-rays having energies of 1173.2 keV and 1332.5 keV) is clearly visible in the calculated dose equivalents. As a result of these simulations, a shielding of 5cm is required.

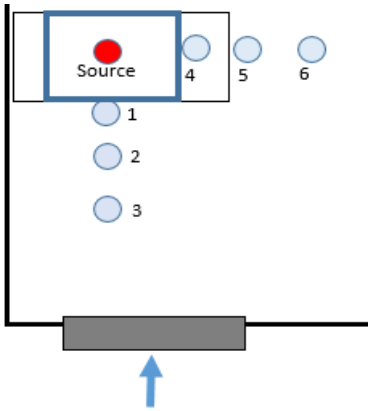

Fig. 3.8 Dose calculation points around the source stocker (grey box indicates the entrance door).

Table 3.2 Equivalent dose H*10 (µSv/h) calculated at various points in the laboratory.

Source	*Position #*	*Dose equivalent H*(10) (µSv/h) with shielding of:*		
		1cm	*3cm*	*5cm*
^{133}Ba (1 GBq)	1	0.25	<0.1	0
	2	<0.1	<0.1	0
	3	<0.1	<0.1	0
	4	<0.1	<0.1	0
	5	<0.1	<0.1	0
	6	<0.1	0	0
^{60}Co (1 GBq)	1	2 477	812	236
	2	435	152	49
	3	130	45	15
	4	563	158	41
	5	220	68	18
	6	89	27	8

Conclusion

The ionisation chamber and associated electronics is now functioning and an initial measurement of the half-life of ^{99m}Tc has been performed. Final analysis is still ongoing in order to ensure the full uncertainty budget is correctly treated.

Simulations have been performed in order to calculate the shielding requirements for the source stocker, which can store a maximum 16 ampoules of radioactive solutions on a carousel. The automatic source displacement device is currently under construction and will be put into service in 2022. The relevant control and analysis software, developed using the Python language, are under final testing. Finalisation of these two aspects will then allow the systematic measurement of half-lives from a range of radionuclides to be undertaken on a routine basis and with minimal human supervision.

References

[1] M.-M. Bé, V. Chisté, C. Dulieu, E. Browne, V. Chechev, N. Kuzmenko, R. Helmer, A. Nichols, E. Schönfeld, R. Dersch, Table of Radionuclides (Vol.1 - A = 1 to 150), Monographie BIPM-5, Vol.1, Bureau International des Poids et Mesures (2004) 183-190

[2] E. Browne and J.K. Tuli, Nuclear Data Sheets for A=99, Nuclear Data Sheets 145 (2017) 25–340

[3] M.P. Unterweger and R. Fitzgerald, Update of NIST half-life results corrected for ionization chamber source-holder instability, Applied Radiation and Isotopes **87** (2014) 92; Erratum Applied Radiation and Isotopes **159** (2020) 108976

[4] J. Sempau, E. Acosta, J. Baro, J.M. Fernandez-Varea, F.Salvat, An algorithm for Monte Carlo simulation of the coupled electron-photon transport. Nuclear Instruments and Methods B 132 (1997) 377-390 and F. Salvat, PENELOPE-2018 - A Code System for Monte Carlo Simulation of Electron and Photon Transport - Workshop Proceedings Barcelona, Spain 28 January - 1 February 2019, NEA/MBDAV/R(2019)1, ISSN 2707-2894, 2019